THE PROTEIN SOCIETY

Recombinant expression, purification, and biophysical characterization of the transmembrane and membrane proximal domains of HIV-1 gp41

Zhen Gong,[1,2] Sarah A. Kessans,[3,4†] Lusheng Song,[5] Katerina Dörner,[1,2] Ho-Hsien Lee,[1,2] Lydia R Meador,[3,4] Joshua LaBaer,[4] Brenda G. Hogue,[3,4] Tsafrir S. Mor,[3,4*] and Petra Fromme[1,2*]

[1]Department of Chemistry and Biochemistry, Arizona State University, Tempe, Arizona 85287-1604

[2]The Center for Applied Structural Discovery, The Biodesign Institute, Arizona State University, Tempe, Arizona 85287

[3]School of Life Sciences, Arizona State University, Tempe, Arizona 85287-4501

[4]The Center for Infectious Diseases and Vaccinology, The Biodesign Institute, Arizona State University, Tempe, Arizona 85287–5401

[5]Virginia G. Piper Center for Personalized Diagnostics, The Biodesign Institute, Arizona State University, Tempe, Arizona 85287-6401

Received 11 March 2014; Revised 22 July 2014; Accepted 20 August 2014
DOI: 10.1002/pro.2540
Published online 23 August 2014 proteinscience.org

Abstract: The transmembrane subunit (gp41) of the envelope glycoprotein of HIV-1 associates non-covalently with the surface subunit (gp120) and together they play essential roles in viral mucosal transmission and infection of target cells. The membrane proximal region (MPR) of gp41 is highly conserved and contains epitopes of broadly neutralizing antibodies. The transmembrane (TM) domain of gp41 not only anchors the envelope glycoprotein complex in the viral membrane but also dynamically affects the interactions of the MPR with the membrane. While high-resolution X-ray structures of some segments of the MPR were solved in the past, they represent the post-fusion forms. Structural information on the TM domain of gp41 is scant and at low resolution. Here we describe the design, expression and purification of a protein construct that includes MPR and the transmembrane domain of gp41 (MPR-$TM_{TEV\text{-}6His}$), which reacts with the broadly neutralizing antibodies 2F5 and 4E10 and thereby may represent an immunologically relevant conformation mimicking a prehairpin intermediate of gp41. The expression level of MPR-$TM_{TEV\text{-}6His}$ was improved

Abbreviations: Ab, antibody; βDDM, n-β-dodecyl-D-maltoside; CD, circular dichroism; CHR, C-terminal heptad repeat region of gp41; CTB, cholera toxin B subunit; CTD, cytoplasmic tail domain of gp41; CV, column volume; DLS, dynamic light scattering; FP, fusion peptide of gp41; FPPR: fusion peptide proximal region of gp41; GalCer, galactosyl ceramide; HIV-1, human immunodeficiency virus type 1; IPTG, isopropyl β-D-1-thiogalactopyranoside; mAb, monoclonal antibody; MPER, membrane proximal external region of gp41; MPR, region of gp41 corresponding to the MPER and part of the CHR; NHR, N-terminal heptad repeat region of gp41; RMSD, root-mean-square deviation; SEC, size exclusion chromatography; SMS, Supplementary Material section; SPR, surface plasmon resonance; TEV, tobacco etch virus; TM, transmembrane domain of gp41.

Additional Supporting Information may be found in the online version of this article.

†Current address: Present address: Private Bag 4800, Biomolecular Interaction Centre, School of Biological Sciences, University of Canterbury, Christchurch 8140, New Zealand

Grant sponsor: Center for Membrane Proteins in Infectious Diseases (MPID), Protein Structure Initiative of NIH PSI:Biology of the National Institute of Health; Grant number: 1U54GM094625.

*Correspondence to: Tsafrir S. Mor, School of Life Sciences and The Biodesign Institute, P.O. Box 874501, Arizona State University, Tempe, AZ 85287-4501. E-mail: tsafrir.mor@asu.edu. Correspondence to: Petra Fromme, Department of Chemistry and Biochemistry, P.O. Box 871604, Arizona State University, Tempe, AZ 85287-1604. E-mail: pfromme@asu.edu

by fusion to the C-terminus of Mistic protein, yielding ~1 mg of pure protein per liter. The isolated MPR-TM$_{TEV-6His}$ protein was biophysically characterized and is a monodisperse candidate for crystallization. This work will enable further investigation into the structure of MPR-TM$_{TEV-6His}$, which will be important for the structure-based design of a mucosal vaccine against HIV-1.

Keywords: HIV-1; gp41; membrane proximal region; transmembrane domain; dynamic light scattering; surface plasmon resonance

Introduction

The envelope glycoprotein of the human immunodeficiency virus type 1 (HIV-1) plays essential roles in virus attachment and fusion with target cells[1] and is also a primary target for vaccine design.[2] It is a complex consisting of two noncovalently associated subunits that are cleaved off their precursor polyprotein to form the surface (gp120) and the transmembrane subunit (gp41).[3] The transmembrane anchor, gp41, consists of an ectodomain (Residues 512–683, Fig. 1), a transmembrane domain (Residues 684–705), and a cytoplasmic domain (Residues 706–856).[3,4] Biophysical and structural studies delineate further distinct structural and functional features within the ectodomain of gp41 (Fig. 1) including the N-terminal and C-terminal heptad repeat regions (NHR and CHR)[3,5,6] that are flanked by the fusion peptide (FP) and the fusion peptide proximal region (FPPR) on one side, and the membrane proximal external region (MPER) on the other side.

Target-cell infection by HIV-1 is initiated when gp120 binds to its primary receptor CD4 and coreceptor, usually CCR5 or CXCR4.[7,8] The exact mechanism leading to virus entry is still not known. A current model proposes that following binding of gp120 to its receptors, the gp41 subunit is exposed, triggering drastic sequential changes in its conformation culminating in fusion between the viral envelope and the target cell's plasma membrane.[9–11] According to this model, NHR and CHR of gp41 are partially shielded by gp120, and switch to an extended conformation upon the latter's removal to allow insertion of the FP into the target cell's membrane.[12–14] After the fusion of the juxtaposed viral and cellular membranes, gp41's core regains the 6-helical bundle conformation of post-fusion complex.[15]

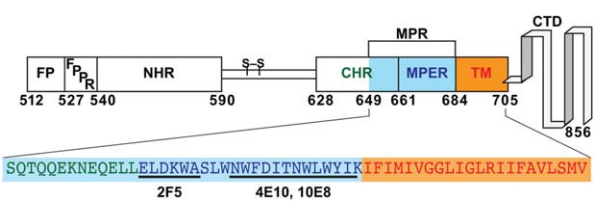

Figure 1. Schematic diagram of HIV-1 gp41. FP (Residues 512–527): fusion peptide; FPPR (Residues 528–539): fusion peptide proximal region; NHR (Residues 540–590): N-terminal heptad repeat region; S-S: a disulfide linkage; CHR (Residues 628–661): C-terminal heptad repeat region; MPER (Residues 662–683): membrane proximal external region; MPR (Residues 649–683): membrane proximal region; TM (Residues 684–705): transmembrane domain; CTD (Residues 706–856): cytoplasmic domain. 2F5, 4E10, and 10E8 are epitopes for three broadly neutralizing mAbs.

In addition to its well-recognized role in infection of target CD4$^+$ cells, gp41 is instrumental during early steps in various processes leading to mucosal transmission of the virus.[16–19] The virus utilizes several routes to cross epithelial surfaces including capture by dendritic and Langerhans cells prevailing in pluristratified epithelia and transcytosis that is particularly important in simple epithelia.[20]

A key player in the transcytosis process is a region of the gp41 corresponding to residues 649–683, which includes the MPER and part of the CHR and will be referred to herein in correspondence with Matoba *et al.*[21] as "MPR". Transcytosis is initiated when the MPR binds to the glycosphingolipid galactosyl ceramide (GalCer) and the co-receptor CCR5.[18,22,23] GalCer is enriched at the apical membrane of epithelial cells[24] and is involved in the establishment of lipid rafts,[25,26] which are proposed to act as platforms for HIV-1 entry,[27] transcytosis,[22] virion assembly, and budding.[28]

The minimal region of gp41 that can bind GalCer is the MPR. This region, together with the adjacent transmembrane domain, is the most highly conserved element of the envelope protein.[3,22,29,30] The MPR is the target of secretory IgAs that can be found in mucosal secretions of highly exposed, persistently seronegative individuals and may constitute one of very few potential correlates of protection against HIV-1 infection.[31–36] These mucosal antibodies (Abs) were shown to possess anti-HIV responses including neutralization and blocking of transcytosis.[31,33] Significantly, epitopes within the MPER are recognized by three of only a handful of broadly neutralizing monoclonal Abs (mAbs) characterized thus far. Among them are 2F5,[37] 4E10,[38] and more recently 10E8.[39] These mAbs also have other anti-HIV-1 activities including transcytosis-blocking[40] and Fc-mediated cytotoxicity[41] and were shown to provide full protection against mucosal challenge when delivered intravenously.[42–44] These attributes make the MPR a particularly interesting target for the development of a prophylactic vaccine against HIV-1.[19,45–49]

Consequently, elucidation of the structure of the MPR is of interest and importance as it will instruct mucosal vaccine design against HIV-1. Liu *et al.*

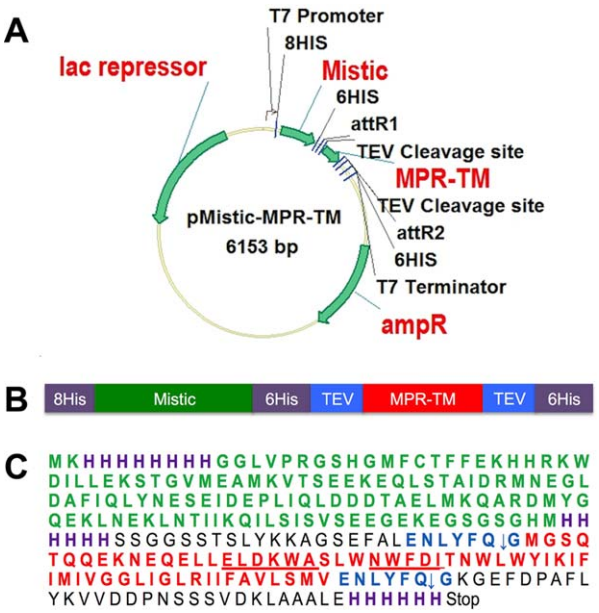

Figure 2. A: Construction of the expression vector for pMistic-MPR-TM$_{TEV\text{-}6His}$. See text and Supporting Information for details. B: Scheme of the Mistic-MPR-TM$_{TEV\text{-}6His}$ fusion protein. C: Amino acid sequence of Mistic-MPR-TM$_{TEV\text{-}6His}$. Purple: His-tag; Green: Mistic; red: MPR-TM; underlined ELDKWA: the mAb 2F5 core epitope; underlined NWFDI: the 4E10 mAb core epitope; blue: TEV recognition sites. Note that the cleavage occurred between Q and G residues of the TEV recognition sequence ENLYFQG.

have reported that a portion of the MPER (Residues 662–683) forms a parallel three-stranded coiled coil stabilized by the addition of a C-terminal isoleucine zipper motif.[12] However, it is difficult to determine whether MPER forms the three-stranded coiled coil by itself or if this MPER is forced into this conformation by its attachment to the three helix bundles with the isoleucine zipper, which forms a classic coiled coil.[50] Instead of using an artificial motif to stabilize MPR, we want to study the structure of MPR together with its native transmembrane domain, which, similarly to the MPR, is highly conserved.[3]

Studies on the function of the transmembrane domain of HIV-1 gp41 are limited. The transmembrane domain of HIV-1 gp41 plays an important role in anchoring the glycoprotein envelope complex into the viral membrane and is also crucial for its biological function in fusion and virus entry.[51–54] Mao *et al.* recently obtained a 6-Å structure of the membrane-bound HIV-1 envelope glycoprotein trimer in its uncleaved state by using cryo-electron microscopy (EM), which included the transmembrane domain of gp41.[55] Their low-resolution structural model proposed that the transmembrane domain of gp41 might form a left-handed three α-helical coiled coil, with a crossing angle of about 35°. This is the only structural information of the transmembrane domain of gp41 reported so far. The structure of MPR-TM at higher resolution is still needed for the structure-based design of a vaccine against HIV-1.

There are two bottlenecks in membrane protein structure determination: high-yield membrane protein production and crystallization. There are two major reasons that account for the difficulty in producing large amounts of correctly-folded membrane proteins in bacteria. Most eukaryotic membrane proteins are inserted into the membrane in a process which combines translation, targeting, folding and post-translational modifications. Despite some similarities and homologous elements, the membrane-targeting pathways in bacteria are different enough to require engineering of eukaryotic genes to optimize their expression and accumulation. In addition, the limited membrane surface area in *Escherichia coli* may not only limit the total amount of properly-folded recombinant proteins made in this system, but also may have cytotoxic consequences by competitively reducing the production of vital host membrane proteins or by negatively affecting membrane physiology.[56] Mistic is a *Bacillus subtilis* integral membrane protein that autonomously folds into the membrane. It acts as a targeting signal and can be used for over-expression of other membrane proteins in their native conformations.[56] In our study, we developed an expression and purification strategy of MPR-TM$_{TEV\text{-}6His}$ fused to the C-terminus of Mistic. Surface plasmon resonance (SPR) measurements and ELISA experiments were carried out to test if the epitope on the purified MPR-TM$_{TEV\text{-}6His}$ was exposed and could be recognized by the broadly neutralizing mAbs 2F5 and 4E10. The purified MPR-TM$_{TEV\text{-}6His}$ was also biophysically characterized by size exclusion chromatography (SEC), MALDI-TOF MS, CD spectroscopy and dynamic light scattering (DLS).

Results and Discussion

Cloning and expression of MPR-TM$_{649–705}$

The membrane proximal region (MPR) of HIV-1 gp41 is important for the design of a mucosal vaccine against HIV-1. The transmembrane (TM) domain of HIV-1 gp41 plays an essential role in anchoring the envelope complex into the viral membrane and is also crucial for its biological function in fusion and virus entry.[51–53] Bacterial expression of these two hydrophobic domains of HIV-1 has proved to be difficult and previous experiments in our laboratories making use of the P8CBD expression vector[57] resulted in extremely poor accumulation of properly-targeted MPR-TM (Gong, Kessans, Fromme and Mor, unpublished). In our study, the portion of the HIV-1 Env gene encoding for MPR-TM was cloned into the expression vector pMIS2.1mv to obtain pMistic-MPR-TM$_{TEV\text{-}6His}$ [Fig. 2(A)]. This vector directs the tightly regulated expression of a C-terminal translation fusion between the

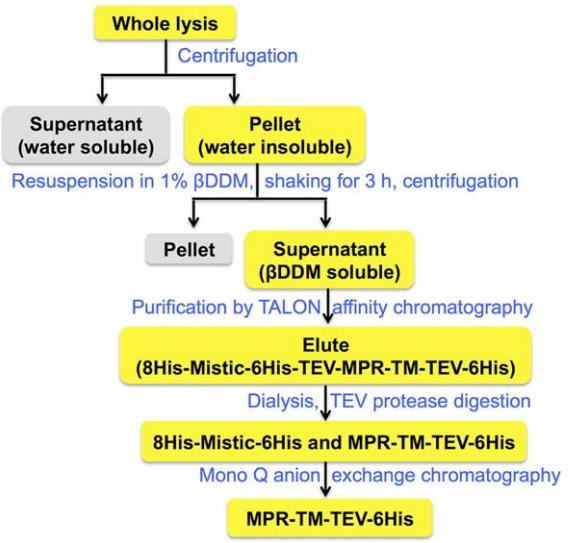

Figure 3. MPR-$TM_{TEV\text{-}6His}$ purification scheme.

B. subtilis integral membrane protein Mistic and MPR-$TM_{TEV\text{-}6His}$ in *E. coli* [Fig. 2(B,C)]. Mistic was previously shown to improve as a translational-fusion partner the expression and accumulation levels of several membrane proteins in their native conformations.[56] To allow the removal of the Mistic fusion partner prior to future crystallization experiments, two tobacco etch virus (TEV) protease recognition sites[58] were introduced by PCR primers. One TEV protease recognition site was introduced at the N-terminus of MPR-$TM_{649–705}$ and the other was located at the C-terminus [Fig. 2(B,C)]. The recombinant plasmid pMistic-MPR-$TM_{TEV\text{-}6His}$ was transformed into *E. coli* C41 (DE3) cells for expression.

Purification of MPR-$TM_{TEV-6His}$

After cells were lysed by microfluidization, the majority of the fusion protein Mistic-MPR-$TM_{TEV\text{-}6His}$ was found in the membrane fraction, and a purification protocol was developed to allow efficient purification without compromising the structural integrity of the protein (Fig. 3). Following extensive screening of various detergents (data not shown), βDDM at 1% was used to extract the fusion protein from the membrane. The βDDM extract was subjected to TALON metal affinity chromatography to separate His-tagged Mistic-MPR-$TM_{TEV\text{-}6His}$ from other proteins.[59,60] The second elution fraction contained the majority of His-tagged proteins, which showed a complex pattern of banding upon SDS-PAGE fractionation (Fig. 4). The very top band (marked with blue arrows) corresponded to the fusion protein Mistic-MPR-$TM_{TEV\text{-}6His}$, with a molecular mass of 31 kDa, in good concordance with its calculated expected size. Four contaminant bands were visible. The second band from the top on the silver-stained SDS-PAGE in Figure 4 corresponded to a His-tagged fragment of Mistic and MPR-$TM_{TEV\text{-}6His}$ as it could be detected in immunoblots by the MPR-specific mAb 2F5 (Fig. 4). In contrast, the three lower bands, clearly visible on the silver-stained gels, did not react with the 2F5 Ab (Fig. 4) and could be His-tagged fragments of Mistic without MPR or unrelated *E. coli* proteins. We observed that degradation was a common problem for Mistic fusion constructs (data not shown).

The next step in our purification scheme (Fig. 3) was the specific cleavage of the fusion protein followed by anion exchange chromatography to separate the MPR-$TM_{TEV\text{-}6His}$ protein from its Mistic fusion partner. The TALON column eluates were dialyzed to remove the imidazole and the ionic conditions of the buffer were adjusted to ensure efficient cleavage by the TEV protease. We expected the fully processed MPR-TM protein to have a molecular weight of 7.8 kDa, if both the N-terminal and C-terminal TEV recognition sites were cleaved. However, extensive digestion by TEV protease yielded a protein band (indicated by red arrows in Fig. 4) with an apparent molecular mass greater than 10 kDa that cross-reacted with the MPR-specific mAb 2F5. Moreover, subjecting the cleavage products to a second TALON purification step demonstrated that this >10 kDa cleavage protein retained a functional His-tag that allowed its efficient binding to the column and required high concentration of imidazole (250 m*M*) for elution (data not shown). Our results are therefore compatible with the lack of TEV cleavage at its C-terminal site of the protein. The final product therefore consists of the MPR-TM with its C-terminal His-tag still attached (called hereafter "MPR-$TM_{TEV\text{-}6His}$"). The expected molecular mass of this polypeptide was 11.9 kDa. Lack of cleavage at the C-terminal TEV recognition site could be

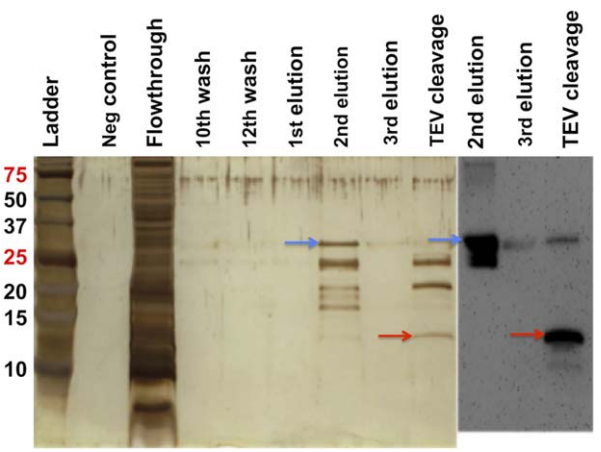

Figure 4. Purification of Mistic-MPR-$TM_{TEV\text{-}6His}$ by metal affinity chromatography and its cleavage by TEV protease. Fractions were resolved by SDS-PAGE and visualized by silver staining (left) or immunoblotting with the mAb 2F5 (right). Blue arrows: Mistic-MPR-$TM_{TEV\text{-}6His}$. Red arrows: cleaved MPR-$TM_{TEV\text{-}6His}$.

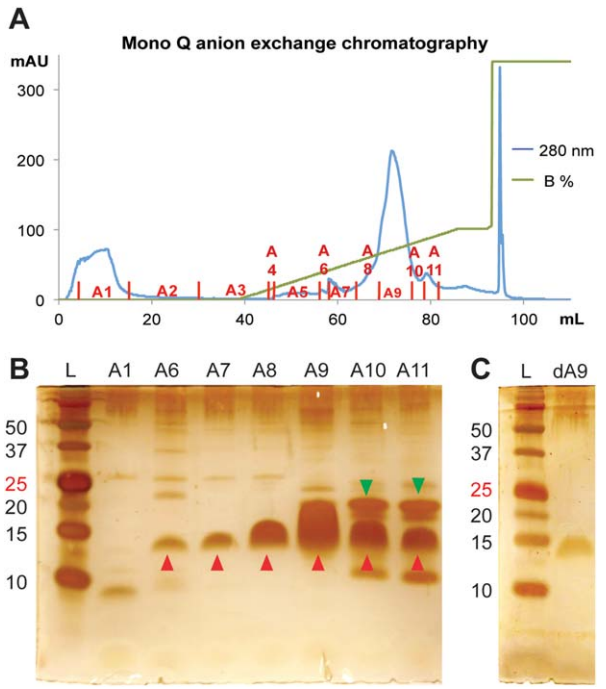

Figure 5. Separation of Mistic-MPR-$TM_{TEV\text{-}6His}$ cleavage products by Mono Q anion exchange chromatography. (A) Chromatogram (B) Fractions were resolved by SDS-PAGE and visualized by silver staining. Red arrowheads: MPR-$TM_{TEV\text{-}6His}$; green arrowheads: $_{8His}Mistic_{6His}$. (C) SDS-PAGE analysis of 10-fold diluted fraction A9 (dA9). L, ladder.

explained by its proximity to TM domain, which is likely to be fully embedded in the detergent micelle, thereby the hydrophilic sugar heads of the βDDM molecules may obscure the TEV cleavage site or may otherwise impede the enzyme's proteolytic activity.

Retention of the C-terminal His-tags on the MPR-$TM_{TEV\text{-}6His}$ protein interfered with our original plan to separate it from the other cleavage products containing the Mistic protein by the second TALON metal-affinity chromatography step. Instead, we turned to size-exclusion chromatography (SEC) and experimented with two types of SEC columns, Superdex 75 10/300 GL and Superdex 200 10/300 GL, to separate MPR-$TM_{TEV\text{-}6His}$ from $_{8His}Mistic_{6His}$ and other degradation products, but MPR-$TM_{TEV\text{-}6His}$ could not be purified by either of the two columns (data not shown).

Finally, Mono Q anion exchange chromatography was used to further purify the MPR-$TM_{TEV\text{-}6His}$ protein. The optimal conditions for Mono Q anion exchange chromatography were chosen based on several prior small-scale tests. MPR-$TM_{TEV\text{-}6His}$ eluted as the main elution peak [A9 in Fig. 5(A)] while $_{8His}Mistic_{6His}$ and other degradation proteins were in the flowthrough [A1 in Fig. 5(A)] and a shoulder peak [A 10 and A11 in Fig. 5(A)] of the main elution peak. The protein elution was monitored at 280 nm and the fractions were analyzed by SDS-PAGE [Fig. 5(B)]. The band labeled by red arrowheads corresponds to MPR-$TM_{TEV\text{-}6His}$ while the band pointed out by green arrowheads corresponds to the cleaved $_{8His}Mistic_{6His}$. Fraction A9 was overloaded so it was very difficult to determine if the strong band was MPR-$TM_{TEV\text{-}6His}$ only or the mixture of $_{8His}Mistic_{6His}$ and MPR-$TM_{TEV\text{-}6His}$. Fraction A9 was diluted 10 times and reanalyzed by SDS-PAGE [Fig. 5(C)]. The result shown in Figure 5(C) confirms that fraction A9 only contains MPR-$TM_{TEV\text{-}6His}$. The protein preparations corresponding to fraction A9 were used for future analysis.

The presence of the uncleaved C-terminal tail containing the C-terminal TEV recognition site, an attR2 site and a 6His-tag [Fig. 2(C)] may raise the concern that it might affect future crystallization of MPR-$TM_{TEV\text{-}6His}$. However, this seems unlikely as the protein data bank (PDB) contains several examples of high-resolution structures containing such an artificial protein domain including a 1.55 Å crystal structure of the thioredoxin domain of human thioredoxin-like protein 2 (PDB: 2WZ9).

Purified MPR-$TM_{TEV-6His}$ is folded and stable

Circular dichroism (CD) spectroscopy was used to estimate the secondary structural content of MPR-$TM_{TEV\text{-}6His}$. The CD spectra of MPR-$TM_{TEV\text{-}6His}$ displayed one positive band at 195 nm and two negative bands at 208 nm and 222 nm (Fig. 6), which is characteristic of α-helical proteins.[61] Data analysis with CONTINLL in the CDPro software package[62] produced an estimation of 52.2% α helices, 6.3% β sheets, 14.9% turns, and 26.5% random coils and the root-mean-square deviation (RMSD) value was 0.055. Estimation with CONTINLL was similar to the secondary structure prediction with server APSSP2,[63] which predicted 59.6% α helices. The 2-Å crystal structure of the $gp41_{528–683}$ indicated that the MPR (Residues 649–683) might form an α-helix.[13] As reported by Mao et al.,[55] the 6-Å cryo-EM

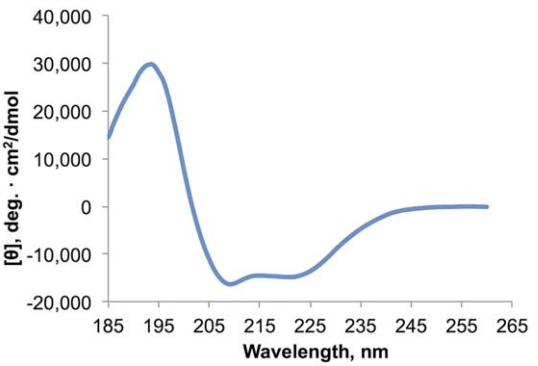

Figure 6. CD spectrometry demonstrated that purified MPR-$TM_{TEV\text{-}6His}$ was α-helical. With one positive band at 195 nm and two negative bands at 208 nm and 222 nm, the CD spectra of the protein were typical for α-helical proteins.

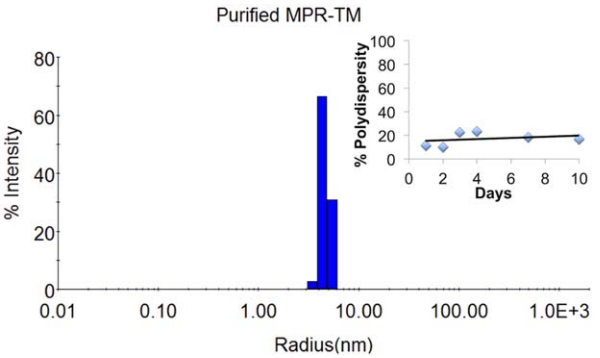

Figure 7. DLS demonstrated that purified MPR-$TM_{TEV\text{-}6His}$ was highly monodisperse. Sample contained MPR-$TM_{TEV\text{-}6His}$ (0.22 mg/mL) in 100 m*M* NaF, 20 m*M* NaH_2PO_4, pH 7.5, 0.02% βDDM. Insert: the purified MPR-$TM_{TEV\text{-}6His}$ was stored at 4°C and measured by DLS at Days 1, 2, 3, 4, 7, and 10, respectively. The polydispersity remained below 25% (please refer to Supporting Information Table 2 and Supporting Information Figure 1 for details), which indicated that purified MPR-$TM_{TEV\text{-}6His}$ was monodisperse for at least 10 days at 4°C.

structure of the uncleaved HIV-1 envelope glycoprotein trimer suggests that the transmembrane domain (Residues 684–705) of gp41 might be an α-helix as is generally assumed (but see Steckbeck *et al*. for a different view[64]). Please note that the Env structure proposed by Mao *et al*.[55] differs from other recent structures based on crystallographic and EM studies, and some aspects of that model remain controversial.[14,65,66] In particular, the organization of secondary structure elements in the gp41 ectodomain of the structure proposed by Mao *et al*.[55] is dramatically different from that of the six α-helix bundles seen in the post-fusion form. Specifically, according to Mao *et al*.,[55] the NHR and CHR domains are broken into eight short α-helices in striking opposition to the six helical bundle. In any event, the CD spectra indicate that MPR-$TM_{TEV\text{-}6His}$ is folded after purification.

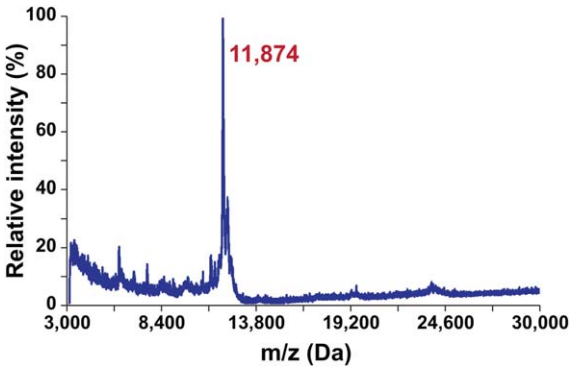

Figure 8. MALDI-TOF spectra of MPR-$TM_{TEV\text{-}6His}$ were in perfect agreement with the calculated molecular mass of the protein at 11,872 Da.

We used dynamic light scattering (DLS) to further demonstrate that purified *E. coli*-derived MPR-$TM_{TEV\text{-}6His}$ is stably folded and monodisperse as these are critical factors affecting crystallization.[67] DLS is a technique that is very sensitive for the detection of aggregates. Our DLS analysis demonstrated that purified MPR-$TM_{TEV\text{-}6His}$ was monodisperse, with polydispersity of the protein-detergent complex estimated to be only 12.3% (Fig. 7 and Supporting Information Table 1). Moreover, we have used DLS to monitor the stability of purified MPR-$TM_{TEV\text{-}6His}$ protein at 4°C over time. Our result shows that MPR-$TM_{TEV\text{-}6His}$ remains monodisperse for at least 10 days at 4°C (Fig. 7 insert, Supporting Information Fig. 1). The DLS results indicate that MPR-$TM_{TEV\text{-}6His}$ is a monodisperse and stable candidate for crystallization.

Molecular mass of MPR-$TM_{TEV-6His}$ and its oligomeric state

We used MALDI-TOF MS to determine the accurate molecular mass of MPR-$TM_{TEV\text{-}6His}$ and the resulting spectrum revealed a protein peak of 11,874 ± 4 Da (Fig. 8). This agreed very well with the theoretical molecular weight of MPR-$TM_{TEV\text{-}6His}$, which was predicted to be 11,872 Da based on the sequence (Fig. 2) and the SDS-PAGE analysis (Fig. 4). The shoulder peak at 12,138 Da could be assigned to the complex of MPR-$TM_{TEV\text{-}6His}$ and the matrix sinapinic acid whose molecular weight was 224 Da.

The MS results confirm the predicted molecular mass of the MPR-$TM_{TEV\text{-}6His}$. Proteins are denatured by MALDI using sinapinic acid and do not provide information about the oligomeric information. It was, therefore, of interest to check the oligomerization state of the purified protein. Our DLS results showed that the Stokes radius of the detergent-protein complex was 4.68 nm, which corresponded to a molecular mass of 124 kDa (Supporting Information Table 1). This indicates that MPR-$TM_{TEV\text{-}6His}$ polypeptides form a larger complex consisting of several monomeric subunits. However, the oligomeric state of the complex is difficult to determine, as it exists in the form of a protein-detergent complex.

We have used analytical SEC to verify the quaternary structure of purified MPR-$TM_{TEV\text{-}6His}$ and to provide an additional estimate as to its molecular mass and its oligomeric state in its detergent-solubilized state (Fig. 9). The SEC chromatogram revealed a single symmetric peak that eluted at 13.70 mL [Fig. 9(A)]. The molecular weight of this peak was ~123 kDa, calculated based on the standard curve [Fig. 9(B)]. This size corresponds to the MPR-$TM_{TEV\text{-}6His}$ oligomer embedded into a βDDM micelle and was very similar to the molecular weight estimation obtained by DLS (124 kDa, Supporting Information Table 1 and Fig. 7).

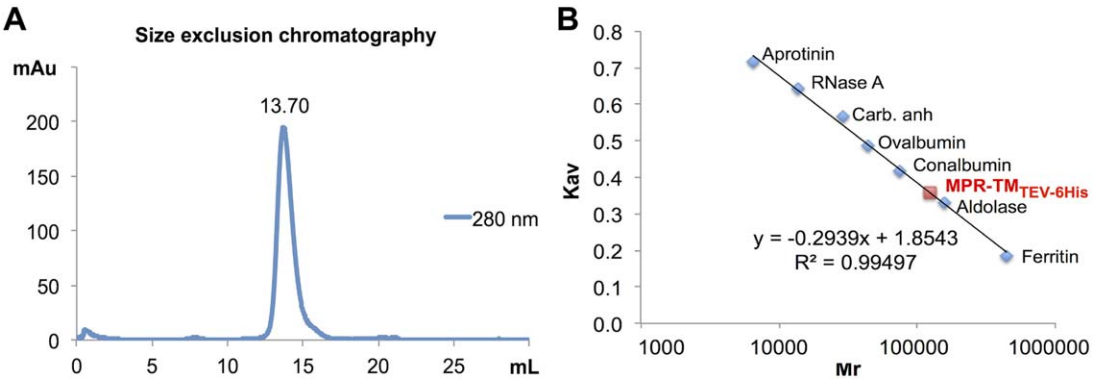

Figure 9. Estimation of the molecular mass of purified native MPR-$TM_{TEV\text{-}6His}$. A: SEC of MPR-$TM_{TEV\text{-}6His}$ revealed a single symmetric peak eluted at 13.7 mL corresponding to ~123 kDa based on the standard curve. B: The standard curve of Superdex 200 10/300 GL column using the following standard proteins: aprotinin (6.5 kDa), RNase A (13.7 kDa), carbonic anhydrase (29 kDa), ovalbumin (43 kDa), conalbumin (75 kDa), aldolase (158 kDa) and ferritin (440 kDa). Kav is the partition coefficient, which can be calculated as following: (elution volume – void volume)/(total volume – void volume).

The excellent correspondence of the DLS and SEC data supported our objective to use the information to assess the oligomeric structure of MPR-$TM_{TEV\text{-}6His}$.The average molecular weight of "empty" βDDM micelles measured by DLS was 68 kDa (data not shown). However, the detergent shell in a protein-detergent complex is often larger than the empty micelle because the detergent must cover all the hydrophobic surface of the protein. Therefore, the estimation of the oligomeric state of the protein inside the micelle is complicated. It is likely that the presence of embedded proteins could change the expected size of the micelle. Other estimates published in the past indicated that detergent to protein ratio values range from 2.4 to 3.5 (g/g).[68,69] A trimer embedded in βDDM micelles could therefore show an apparent molecular mass in the range of 121–160 kDa. In either case, the values for a dimer (81–107 kDa) would be lower than the observed value. While the definitive subunit composition of the MPR-$TM_{TEV\text{-}6His}$ is hard to resolve at this stage, it is clear that the protein is oligomeric, an important structure-function attribute of the native gp41 molecule.

Purified MPR-$TM_{TEV-6His}$ is recognized by the broadly neutralizing mAbs 2F5 and 4E10

An important structure-function attribute of gp41 is its ability to bind to broadly neutralizing mAbs. It was therefore of great importance to test if the deconstructed version of the transmembrane subunit of the envelope protein could be recognized by the broadly neutralizing mAbs 2F5 and 4E10. The 2F5 and 4E10 mAbs interact with a highly conserved sequence of MPER. This part is "hidden" inside a tight helix bundle in most of the structural models reported from MPER.[12,13] Only one structure has been solved containing a shortened NHR (HR1) region, which left MPER accessible to 2F5 Abs.[14] We used ELISA to determine if the 2F5 Ab was able to bind to purified MPR-$TM_{TEV\text{-}6His}$ in its nondenatured state (Fig. 10). The results [Fig 10(A), rows C and D] clearly indicate that the MPR-$TM_{TEV\text{-}6His}$ protein is indeed recognized by the 2F5 Abs. As expected, a positive control consisting of a fusion protein of the cholera toxin subunit B with MPR also reacted with the 2F5 Abs [CTB-MPR, Fig. 10(A), rows E and F]. CTB-MPR has previously been shown to react with 2F5 Abs[48] and was able to elicit Abs that could block the transcytosis progression of HIV through the tight epithelia models.[48] In CTB-MPR, the pentameric nature of CTB is thought to hinder MPR from assuming the trimeric post-fusion conformation that does not allow for antibody access to the 2F5-binding site.[70]

To affirm the ELISA results and to quantitatively assess the affinity of MPR-$TM_{TEV\text{-}6His}$ to the two broadly neutralizing Abs 2F5 and 4E10, we employed SPR measurements [Fig. 10(B,C) and Table I]. The results demonstrate very high affinity (nanomolar and subnanomolar range) of the MPR in the context of its transmembrane domain [MPR-$TM_{TEV\text{-}6His}$, Fig. 10(B)] and as a fusion protein with CTB [Fig. 10(C)], in good agreement with our previously published results concerning CTB-MPR.[47] The calculated dissociation constant (K_D) of 2F5 from MPR-$TM_{TEV\text{-}6His}$ and CTB-MPR was 2.2 ± 0.2 nM and 0.8 ± 0.2 nM, respectively. The calculated dissociation constant (K_D) of 4E10 from MPR-$TM_{TEV\text{-}6His}$ and CTB-MPR was 2.1 ± 0.0 nM and 0.5 ± 0.2 nM, respectively. As a negative control, we tested CTB by itself, which showed no appreciable binding to either 2F5 or 4E10 (data not shown).

The ELISA and SPR results indicated that the 2F5 and 4E10 epitopes in MPR-$TM_{TEV\text{-}6His}$ were exposed and accessible for strong 2F5 and 4E10 binding. These results are in excellent agreement with experiments of other groups aimed at

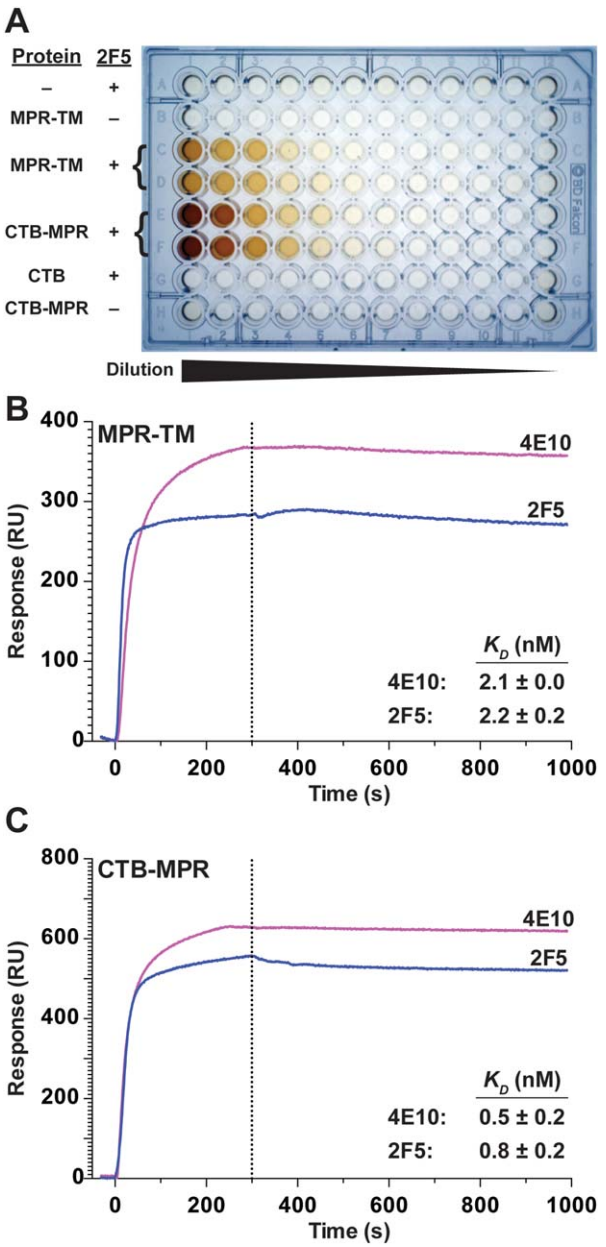

Figure 10. Purified native MPR-$TM_{TEV\text{-}6His}$ can bind to 2F5 and 4E10 mAbs. A: Image of the developed ELISA plate. Row A: control uncoated wells. Rows B-D: wells coated with serially diluted MPR-$TM_{TEV\text{-}6His}$. Rows E, F, and H: wells coated with serially-diluted CTB-MPR. Row G: wells coated with serially-diluted CTB. All rows except B and H were overlaid with the mAb 2F5. (B, C) SPR analysis. Association/dissociation traces of MPR-$TM_{TEV\text{-}6His}$ (B) and CTB-MPR (C) with either 2F5 or 4E10 mAbs. Traces are average of four independent measurements and the dissociation constants (K_D) are listed in the inserts (mean ± SD).

recreating an early fusion intermediate in which the epitopes of 2F5 and 4E10 are exposed to allow interactions with the two neutralizing mAbs (e.g., see Refs. 71–75). For example, Frey *et al.*[75] created a prehairpin intermediate consisting of a trimerization tag fused to the MPER, and to the NHR sandwiched between a duplicated CHR. The NHR was apparently prevented from masking the MPER, thus allowing its interactions with 2F5. More recently, Lutje Hulsik *et al.*[74] have used an even simpler construct that contained the TM domain of gp41, the MPER and the CHR to demonstrate similar high affinities to several neutralizing mAbs. Our construct contains no artificial trimerizing fusion partners, and contains only the C-terminal half of the CHR.

In contrast, both Frey *et al.* and Lutje-Hulsik *et al.*,[74,75] as well as others, demonstrated that gp41 in its prefusion conformation (present on the virions, for example see Ref. 76) cannot interact with 2F5 or 4E10 prior to Env's interactions with the CD4 receptor.[76,77] Similarly, a post-fusion conformation precludes 2F5 and 4E10 binding.[74,75] For example, Liu *et al.*[12] reported a tight helix bundle structure for MPER. In their study, MPER of gp41 was fused to a trimeric C-terminal isoleucine zipper motif and formed a parallel three-stranded coiled coil. The 2F5 epitopes were buried within the interface between the MPER helices and could not be recognized by 2F5.[12] Our results provide further experimental evidence of the importance of the transmembrane domain of gp41 to preserve the immunological signature of the membrane proximal region of gp41,[54] probably mimicking a prehairpin intermediate. It also demonstrates the need to remove the heptad repeat regions.

In summary, we describe here the design, expression, and purification of a protein construct that includes MPR and the transmembrane domain of gp41 (MPR-$TM_{TEV\text{-}6His}$), which reacts with the broadly neutralizing Abs 2F5 and 4E10 and thereby may represent an immunologically relevant conformation mimicking a prehairpin intermediate of gp41. The quantity and quality of purified MPR-$TM_{TEV\text{-}6His}$ reported here make the protein suitable for crystallization experiments and NMR studies as a prerequisite for structural studies, which may guide the structure-based design of vaccines against HIV-1 in the future.

Materials and Methods

Cloning, bacterial strains, and growth conditions

The MPR-$TM_{649–705}$ construct is based on a deconstructed HIV-1 gp41 (dgp41) gene (GenBank Accession number JX534518),[78] a chimera comprising the gp41 MPR derived from the B-clade MN isolate (GenBank accession number AF075722) and the transmembrane domain and cytoplasmic tail region of the C clade 1084i isolate (GenBank accession number AY805330). A more detailed description can be found in the online Supplementary Material section (SMS). Briefly, two tobacco etch virus (TEV) protease recognition sites were added to flank the coding sequence of MPR-$TM_{649–705}$ and the construct

Table I. *Association and Dissociation Rate Constants Derived from SPR Analysis*

Immobilized ligand	Flowing analyte	k_a, ms^{-1}	k_d, s^{-1}	K_D, M
2F5	MPR-TM	4.7 ± 0.3 E4	9.9 ± 0.1 E-5	2.2 ± 0.2 E-9
4E10	MPR-TM	2.3 ± 0.1 E4	5.0 ± 0.4 E-5	2.1 ± 0.0 E-9
2F5	CTB-MPR	5.5 ± 0.7 E4	4.2 ± 1.0 E-5	0.8 ± 0.2 E-9
4E10	CTB-MPR	4.7 ± 0.3 E4	2.5 ± 1.3 E-5	0.5 ± 0.2 E-9

was introduced into a Gateway entry vector pCR8/GW/TOPO (Invitrogen). The construct was then fused to the *B. subtilis* Mistic protein by recombination into the Gateway destination vector pMistic (DNASU: pMIS2.1mv), which was a kind gift of Dr. Mark Vega, Salk Institute. For expression, the recombinant plasmid pMistic-MPR-$TM_{649–705}$ was transformed into *E. coli* C41 (DE3). Cell culture growth conditions and recombinant protein induction are described in the SMS.

Purification of MPR-$TM_{TEV-6His}$

The purification protocol is described in detail in the SMS and will be only outlined here. Harvested cells were lysed with a microfluidizer (Microfluidics). Water-soluble proteins were separated from membrane proteins (and other water-insoluble material) by centrifugation and discarded. The Mistic-MPR-$TM_{TEV-6His}$ fusion protein was extracted by resuspending the pellet in ice-cold extraction buffer (PBS, 1% βDDM and protease inhibitor cocktail) and incubation with gentle shaking for 3 h at 4°C. Following centrifugation, the supernatant was collected and the protein was purified by TALON metal affinity chromatography (Clontech Laboratories, see SMS for details). The eluate was dialyzed (2000 Da cut-off dialysis tube, Sigma) overnight at 4°C against 20 mM NaCl, 20 mM HEPES, pH 7.5. After dialysis, Tris-HCl pH 8.0, EDTA and DTT were added to the dialyzed protein (final concentrations: 50 m*M*, 0.5 m*M*, and 1 m*M*, respectively). The protein preparation was proteolytically digested with TEV protease (Invitrogen, protease:substrate ratio of 20 U/182 μg, 2 h at room temperature) resulting in >95% cleavage of Mistic-MPR-$TM_{TEV-6His}$.

The cleaved MPR-$TM_{TEV-6His}$ protein preparation was further purified by anion exchange chromatography using an ÄKTApurifier 10 (GE Healthcare) and a Mono Q 5/50 GL column (see SMS for details). Fractions containing cleaved MPR-$TM_{TEV-6His}$ were pooled together for further biochemical and biophysical analysis.

Size exclusion chromatography

The purified MPR-$TM_{TEV-6His}$ preparations were characterized by SEC using an ÄKTApurifier 10 (GE Healthcare) and a Superdex 200 10/300 GL column (24 mL bed volume, GE Healthcare). The CD spectroscopy-compatible mobile phase was 100 m*M* NaF, 20 m*M* NaH_2PO_4, pH 7.5, 0.02% βDDM as previously described[47] and as detailed in the SMS.

Protein determination, SDS-PAGE, immunoblotting, and ELISA

Protein determination in crude and enriched preparations was carried out by the modified Lowry assay.[79] Protein concentration of pure preparations of MPR-$TM_{TEV-6His}$ was determined by measuring A_{280} ($\varepsilon = 32{,}290\ cm^{-1}M^{-1}$, obtained using Peptide Property Calculator at http://www.basic.northwestern.edu/biotools/proteincalc.html).

Proteins were separated by SDS-PAGE[80] and were subjected to silver staining[81] or to immunoblotting (see SMS for details).[78] The authors thank the NIH AIDS Research and Reference Reagent Program (Divisions of AIDS, NIAID, NIH) for donation of the mAbs 2F5 (catalog number 1475) and 4E10 (catalog number 10091). Chemiluminescence was detected using the BioSpectrum 500 C Imaging System (Ultra-Violet Products Ltd). ELISA was performed essentially as previously described[47] and as detailed in the SMS.

MALDI-TOF MS, CD spectroscopy, and DLS

We used MALDI-TOF MS (Applied Biosystems) to accurately measure the molecular weight of the purified MPR-$TM_{TEV-6His}$ protein as detailed in the SMS.

A JASCO J-710 CD spectropolarimeter was used for measuring the CD spectra of purified sample and the procedure, detailed in the SMS, was essentially according to Greenfield.[61] Data analysis was performed using the CONTINLL program in CDPro software package by comparing the measured data with reference set option 10, which included 13 membrane proteins along with 43 soluble proteins.[62]

DynaPro NanoStar M3300 from Wyatt Technology was used to carry out DLS measurements in the same buffer used for CD spectroscopy (see the SMS for details).

Surface plasmon resonance (SPR)

All experiments were performed on a K_X5 Surface Plasmon Resonance Imaging (SPRi) System (Plexera). The Kx5 SPRi procedure was previously described[82] and is detailed in the SMS. Preparation of custom SPRi chips is described in the SMS. We used gold chips coated with covalently linked Protein A/G that allowed immobilization of the test Abs through their Fc region, ensuring unimpeded

interactions with antigens. To prevent nonspecific adsorption, the chip was blocked with BSA (5 mg/mL) before further analysis. The running buffer and dilution buffer of the analyte was 1xPBS containing 0.02% βDDM. In sequential runs, CTB (the negative control) at 850 n*M*, CTB-MPR at 600 n*M* and MPR-$TM_{TEV\text{-}6His}$ at 840 n*M* were passed over the ligand surface at a flow rate of 1 μL/s, with a 300-s association and a 600-s dissociation. The chip was regenerated between runs with H_3PO_4 (1 : 200 of 85% w/w) for 100 s followed by recoating with the desired antibody. Identical injections over blank protein A/G surfaces were subtracted from the data for kinetic analysis. SPRi data consisting of video images at 1-s resolution were analyzed with Data Analysis Module software from Plexera. The binding curve was analyzed and fitted with 1:1 interaction model with Scrubber 2 software (Biologic Software).

Acknowledgments

The authors would also like to acknowledge Sasha Daskalova (The Biodesign Institute, Arizona State University) for useful discussion about the creation of the expression vector.

References

1. Hughson FM (1997) Enveloped viruses: A common mode of membrane fusion? Curr Biol 7:R565–R569.
2. Burton DR, Desrosiers RC, Doms RW, Koff WC, Kwong PD, Moore JP, Nabel GJ, Sodroski J, Wilson IA, Wyatt RT (2004) HIV vaccine design and the neutralizing antibody problem. Nat Immunol 5:233–236.
3. Checkley MA, Luttge BG, Freed EO (2011) HIV-1 envelope glycoprotein biosynthesis, trafficking, and incorporation. J Mol Biol 410:582–608.
4. Weiss CD (2003) HIV-1 gp41: mediator of fusion and target for inhibition. AIDS Rev 5:214–221.
5. Chan DC, Fass D, Berger JM, Kim PS (1997) Core structure of gp41 from the HIV envelope glycoprotein. Cell 89:263–273.
6. Weissenhorn W, Dessen A, Harrison SC, Skehel JJ, Wiley DC (1997) Atomic structure of the ectodomain from HIV-1 gp41. Nature 387:426–430.
7. Broder CC, Dimitrov DS (1996) HIV and the 7-transmembrane domain receptors. Pathobiology 64: 171–179.
8. Moore JP, Trkola A, Dragic T (1997) Co-receptors for HIV-1 entry. Curr Opin Immunol 9:551–562.
9. Ashkenazi A, Shai Y (2011) Insights into the mechanism of HIV-1 envelope induced membrane fusion as revealed by its inhibitory peptides. Eur Biophys J 40: 349–357.
10. Melikyan GB (2008) Common principles and intermediates of viral protein-mediated fusion: the HIV-1 paradigm. Retrovirology 5:111.
11. Gallo SA, Finnegan CM, Viard M, Raviv Y, Dimitrov A, Rawat SS, Puri A, Durell S, Blumenthal R (2003) The HIV Env-mediated fusion reaction. Biochim Biophys Acta 1614:36–50.
12. Liu J, Deng Y, Dey AK, Moore JP, Lu M (2009) Structure of the HIV-1 gp41 membrane-proximal ectodomain region in a putative prefusion conformation. Biochemistry (Mosc) 48:2915–2923.
13. Buzon V, Natrajan G, Schibli D, Campelo F, Kozlov MM, Weissenhorn W (2010) Crystal structure of HIV-1 gp41 including both fusion peptide and membrane proximal external regions. PLoS Pathog 6:e1000880.
14. Shi W, Bohon J, Han DP, Habte H, Qin Y, Cho MW, Chance MR (2010) Structural characterization of HIV gp41 with the membrane-proximal external region. J Biol Chem 285:24290–24298.
15. Chan DC, Kim PS (1998) HIV entry and its inhibition. Cell 93:681–684.
16. Shen R, Richter HE, Smith PD (2011) Early HIV-1 target cells in human vaginal and ectocervical mucosa. Am J Reprod Immunol 65:261–267.
17. Wu L (2008) Biology of HIV mucosal transmission. Curr Opin HIV AIDS 3:534–540.
18. Puryear WB, Gummuluru S (2013) Role of glycosphingolipids in dendritic cell-mediated HIV-1 trans-infection. Adv Exp Med Biol 762:131–153.
19. Bomsel M, Tudor D, Drillet AS, Alfsen A, Ganor Y, Roger MG, Mouz N, Amacker M, Chalifour A, Diomede L, Devillier G, Cong Z, Wei Q, Gao H, Qin C, Yang GB, Zurbriggen R, Lopalco L, Fleury S (2011) Immunization with HIV-1 gp41 subunit virosomes induces mucosal antibodies protecting nonhuman primates against vaginal SHIV challenges. Immunity 34:269–280.
20. Ganor Y, Bomsel M (2011) HIV-1 transmission in the male genital tract. Am J Reprod Immunol 65:284–291.
21. Matoba N, Geyer BC, Kilbourne J, Alfsen A, Bomsel M, Mor TS (2006) Humoral immune responses by prime-boost heterologous route immunizations with CTB-MPR(649–684), a mucosal subunit HIV/AIDS vaccine candidate. Vaccine 24:5047–5055.
22. Alfsen A, Bomsel M (2002) HIV-1 gp41 envelope residues 650–685 exposed on native virus act as a lectin to bind epithelial cell galactosyl ceramide. J Biol Chem 277:25649–25659.
23. Meng G, Wei X, Wu X, Sellers MT, Decker JM, Moldoveanu Z, Orenstein JM, Graham MF, Kappes JC, Mestecky J, Shaw GM, Smith PD (2002) Primary intestinal epithelial cells selectively transfer R5 HIV-1 to CCR5+ cells. Nat Med 8:150–156.
24. Simons K, van Meer G (1988) Lipid sorting in epithelial cells. Biochemistry 27:6197–6202.
25. Rietveld A, Simons K (1998) The differential miscibility of lipids as the basis for the formation of functional membrane rafts. BBA-Rev Biomembranes 1376:467–479.
26. Brown DA, London E (1998) Functions of lipid rafts in biological membranes. Annu Rev Cell Dev Biol 14:111–136.
27. Popik W, Alce TM, Au WC (2002) Human immunodeficiency virus type 1 uses lipid raft-colocalized CD4 and chemokine receptors for productive entry into CD4(+) T cells. J Virol 76:4709–4722.
28. Hollmann A, Matos PM, Augusto MT, Castanho MA, Santos NC (2013) Conjugation of cholesterol to HIV-1 fusion inhibitor C34 increases peptide-membrane interactions potentiating its action. PLoS One 8:e60302.
29. Alfsen A, Iniguez P, Bouguyon E, Bomsel M (2001) Secretory IgA specific for a conserved epitope on gp41 envelope glycoprotein inhibits epithelial transcytosis of HIV-1. J Immunol 166:6257–6265.
30. Miyauchi K, Komano J, Yokomaku Y, Sugiura W, Yamamoto N, Matsuda Z (2005) Role of the specific amino acid sequence of the membrane-spanning domain of human immunodeficiency virus type 1 in membrane fusion. J Virol 79:4720–4729.
31. Devito C, Broliden K, Kaul R, Svensson L, Johansen K, Kiama P, Kimani J, Lopalco L, Piconi S, Bwayo JJ,

Plummer F, Clerici M, Hinkula J (2000) Mucosal and plasma IgA from HIV-1-exposed uninfected individuals inhibit HIV-1 transcytosis across human epithelial cells. J Immunol 165:5170–5176.
32. Devito C, Hinkula J, Kaul R, Lopalco L, Bwayo JJ, Plummer F, Clerici M, Broliden K (2000) Mucosal and plasma IgA from HIV-exposed seronegative individuals neutralize a primary HIV-1 isolate. AIDS 14:1917–1920.
33. Tudor D, Derrien M, Diomede L, Drillet AS, Houimel M, Moog C, Reynes JM, Lopalco L, Bomsel M (2009) HIV-1 gp41-specific monoclonal mucosal IgAs derived from highly exposed but IgG-seronegative individuals block HIV-1 epithelial transcytosis and neutralize CD4(+) cell infection: an IgA gene and functional analysis. Mucosal Immunol 2:412–426.
34. Miyazawa M, Lopalco L, Mazzotta F, Lo Caputo S, Veas F, Clerici M (2009) The 'immunologic advantage' of HIV-exposed seronegative individuals. AIDS 23:161–175.
35. Mayr A, Stickl H, Muller HK, Danner K, Singer H (1978) [The smallpox vaccination strain MVA: marker, genetic structure, experience gained with the parenteral vaccination and behavior in organisms with a debilitated defence mechanism (author's transl)]. Zentralbl Bakteriol B 167:375–390.
36. Trabattoni D, Biasin M, Clerici M (2012) Mucosal immunoglobulin A in HIV-exposed seronegative individuals. AIDS 26:2247–2250.
37. Purtscher M, Trkola A, Gruber G, Buchacher A, Predl R, Steindl F, Tauer C, Berger R, Barrett N, Jungbauer A, et al. (1994) A broadly neutralizing human monoclonal antibody against gp41 of human immunodeficiency virus type 1. AIDS Res Hum Retroviruses 10:1651–1658.
38. Zwick MB, Labrijn AF, Wang M, Spenlehauer C, Saphire EO, Binley JM, Moore JP, Stiegler G, Katinger H, Burton DR, Parren PW (2001) Broadly neutralizing antibodies targeted to the membrane-proximal external region of human immunodeficiency virus type 1 glycoprotein gp41. J Virol 75:10892–10905.
39. Huang J, Ofek G, Laub L, Louder MK, Doria-Rose NA, Longo NS, Imamichi H, Bailer RT, Chakrabarti B, Sharma SK, Alam SM, Wang T, Yang Y, Zhang B, Migueles SA, Wyatt R, Haynes BF, Kwong PD, Mascola JR, Connors M (2012) Broad and potent neutralization of HIV-1 by a gp41-specific human antibody. Nature 491:406–412.
40. Shen R, Drelichman ER, Bimczok D, Ochsenbauer C, Kappes JC, Cannon JA, Tudor D, Bomsel M, Smythies LE, Smith PD (2010) GP41-specific antibody blocks cell-free HIV type 1 transcytosis through human rectal mucosa and model colonic epithelium. J Immunol 184: 3648–3655.
41. Tudor D, Bomsel M (2011) The broadly neutralizing HIV-1 IgG 2F5 elicits gp41-specific antibody-dependent cell cytotoxicity in a FcgammaRI-dependent manner. AIDS 25:751–759.
42. Baba TW, Liska V, Hofmann-Lehmann R, Vlasak J, Xu W, Ayehunie S, Cavacini LA, Posner MR, Katinger H, Stiegler G, Bernacky BJ, Rizvi TA, Schmidt R, Hill LR, Keeling ME, Lu Y, Wright JE, Chou TC, Ruprecht RM (2000) Human neutralizing monoclonal antibodies of the IgG1 subtype protect against mucosal simian-human immunodeficiency virus infection. Nat Med 6: 200–206.
43. Mascola JR, Stiegler G, VanCott TC, Katinger H, Carpenter CB, Hanson CE, Beary H, Hayes D, Frankel SS, Birx DL, Lewis MG (2000) Protection of macaques against vaginal transmission of a pathogenic HIV- 1/SIV chimeric virus by passive infusion of neutralizing antibodies. Nat Med 6:207–210.
44. Hessell AJ, Rakasz EG, Tehrani DM, Huber M, Weisgrau KL, Landucci G, Forthal DN, Koff WC, Poignard P, Watkins DI, Burton DR (2010) Broadly neutralizing monoclonal antibodies 2F5 and 4E10 directed against the human immunodeficiency virus type 1 gp41 membrane-proximal external region protect against mucosal challenge by simian-human immunodeficiency virus SHIVBa-L. J Virol 84:1302–1313.
45. Burton DR, Ahmed R, Barouch DH, Butera ST, Crotty S, Godzik A, Kaufmann DE, McElrath MJ, Nussenzweig MC, Pulendran B, Scanlan CN, Schief WR, Silvestri G, Streeck H, Walker BD, Walker LM, Ward AB, Wilson IA, Wyatt R (2012) A blueprint for HIV vaccine discovery. Cell Host Microbe 12:396–407.
46. Matoba N, Kajiura H, Cherni I, Doran JD, Alfsen A, Bomsel M, Fujiyama K, Mor TS (2009) Biochemical and immunological characterization of the plant-derived candidate HIV-1 mucosal vaccine CTB $MPR_{649-684}$. Plant Biotechnol J 7:129–145.
47. Matoba N, Griffin TA, Mittman M, Doran JD, Alfsen A, Montefiori DC, Hanson CV, Bomsel M, Mor TS (2008) Transcytosis-blocking abs elicited by an oligomeric immunogen based on the membrane proximal region of HIV-1 gp41 target non-neutralizing epitopes. Curr HIV Res 6:218–229.
48. Matoba N, Magerus A, Geyer BC, Zhang Y, Muralidharan M, Alfsen A, Arntzen CJ, Bomsel M, Mor TS (2004) A mucosally targeted subunit vaccine candidate eliciting HIV-1 transcytosis-blocking Abs. Proc Natl Acad Sci USA 101:13584–13589.
49. Leroux-Roels G, Maes C, Clement F, van Engelenburg F, van den Dobbelsteen M, Adler M, Amacker M, Lopalco L, Bomsel M, Chalifour A, Fleury S (2013) Randomized phase I: Safety, immunogenicity and mucosal antiviral activity in young healthy women vaccinated with HIV-1 Gp41 P1 peptide on virosomes. PLoS One 8:e55438.
50. Harbury PB, Kim PS, Alber T (1994) Crystal structure of an isoleucine-zipper trimer. Nature 371:80–83.
51. Shang L, Hunter E (2010) Residues in the membrane-spanning domain core modulate conformation and fusogenicity of the HIV-1 envelope glycoprotein. Virology 404:158–167.
52. Shang L, Yue L, Hunter E (2008) Role of the membrane-spanning domain of human immunodeficiency virus type 1 envelope glycoprotein in cell-cell fusion and virus infection. J Virol 82:5417–5428.
53. Yue L, Shang L, Hunter E (2009) Truncation of the membrane-spanning domain of human immunodeficiency virus type 1 envelope glycoprotein defines elements required for fusion, incorporation, and infectivity. J Virol 83:11588–11598.
54. Montero M, Gulzar N, Klaric KA, Donald JE, Lepik C, Wu S, Tsai S, Julien JP, Hessell AJ, Wang S, Lu S, Burton DR, Pai EF, Degrado WF, Scott JK (2012) Neutralizing epitopes in the membrane-proximal external region of HIV-1 gp41 are influenced by the transmembrane domain and the plasma membrane. J Virol 86: 2930–2941.
55. Mao Y, Wang L, Gu C, Herschhorn A, Desormeaux A, Finzi A, Xiang SH, Sodroski JG (2013) Molecular architecture of the uncleaved HIV-1 envelope glycoprotein trimer. Proc Natl Acad Sci USA 110:12438–12443.
56. Roosild TP, Greenwald J, Vega M, Castronovo S, Riek R, Choe S (2005) NMR structure of Mistic, a membrane-integrating protein for membrane protein expression. Science 307:1317–1321.

57. Luo J, Choulet J, Samuelson JC (2009) Rational design of a fusion partner for membrane protein expression in *E*. coli. Protein Sci 18:1735–1744.
58. Parks TD, Leuther KK, Howard ED, Johnston SA, Dougherty WG (1994) Release of proteins and peptides from fusion proteins using a recombinant plant virus proteinase. Anal Biochem 216:413–417.
59. Porath J, Carlsson J, Olsson I, Belfrage G (1975) Metal chelate affinity chromatography, a new approach to protein fractionation. Nature 258:598–599.
60. Hochuli E, Dobeli H, Schacher A (1987) New metal chelate adsorbent selective for proteins and peptides containing neighboring histidine-residues. J Chromatogr 411:177–184.
61. Greenfield NJ (2006) Using circular dichroism spectra to estimate protein secondary structure. Nature Protoc 1:2876–2890.
62. Sreerama N, Woody RW (2000) Estimation of protein secondary structure from circular dichroism spectra: comparison of CONTIN, SELCON, and CDSSTR methods with an expanded reference set. Anal Biochem 287: 252–260.
63. Raghava GPS (2002) APSSP2: A combination method for protein secondary structure prediction based on neural network and example based learning. CASP5: A–132.
64. Steckbeck JD, Sun C, Sturgeon TJ, Montelaro RC (2013) Detailed topology mapping reveals substantial exposure of the "cytoplasmic" C-terminal tail (CTT) sequences in HIV-1 Env proteins at the cell surface. PLoS One 8:e65220.
65. Buzon V, Natrajan G, Schibli D, Campelo F, Kozlov MM, Weissenhorn W (2010) Crystal structure of HIV-1 gp41 including both fusion peptide and membrane proximal external regions. Plos Pathog 6.
66. Lyumkis D, Julien JP, de Val N, Cupo A, Potter CS, Klasse PJ, Burton DR, Sanders RW, Moore JP, Carragher B, Wilson IA, Ward AB (2013) Cryo-EM structure of a fully glycosylated soluble cleaved HIV-1 envelope trimer. Science 342:1484–1490.
67. Ferré-D′Amaré AR, Burley SK (1997) Dynamic light scattering in evaluating crystallizability of macromolecules. Methods Enzymol 276:157–166.
68. Bamber L, Harding M, Butler PJ, Kunji ER (2006) Yeast mitochondrial ADP/ATP carriers are monomeric in detergents. Proc Natl Acad Sci USA 103:16224–16229.
69. Butler PJ, Ubarretxena-Belandia I, Warne T, Tate CG (2004) The *Escherichia coli* multidrug transporter EmrE is a dimer in the detergent-solubilised state. J Mol Biol 340:797–808.
70. Lee H-H, Cherni I, Yu H, Fromme R, Doran JD, Grotjohann I, Mittman M, Basu S, Deb A, Dörner K, Aquila A, Barty A, Boutet S, Chapman HN, Doak RB, Hunter MS, James D, Kirian RA, Kupitz C, Lawrence RM, Liu H, Nass K, Schlichting I, Schmidt KE, Seibert MM, Shoeman RL, Spence JCH, Stellato F, Weierstall U, Williams GJ, Yoon C, Wang D, Zatsepin NA, Hogue BG, Matoba N, Fromme P, Mor TS (In press) Expression, purification and crystallization of CTB-MPR, a candidate mucosal vaccine component against HIV-1. IUCrJ 1. doi:10.1107/S2052252514014900.
71. Kim M, Qiao Z, Yu J, Montefiori D, Reinherz EL (2007) Immunogenicity of recombinant human immunodeficiency virus type 1-like particles expressing gp41 derivatives in a pre-fusion state. Vaccine 25:5102–5114.
72. Qiao ZS, Kim M, Reinhold B, Montefiori D, Wang JH, Reinherz EL (2005) Design, expression, and immunogenicity of a soluble HIV trimeric envelope fragment adopting a prefusion gp41 configuration. J Biol Chem 280:23138–23146.
73. Wang J, Tong P, Lu L, Zhou L, Xu L, Jiang S, Chen YH (2011) HIV-1 gp41 core with exposed membrane-proximal external region inducing broad HIV-1 neutralizing antibodies. PLoS One 6:e18233.
74. Lutje Hulsik D, Liu YY, Strokappe NM, Battella S, El Khattabi M, McCoy LE, Sabin C, Hinz A, Hock M, Macheboeuf P, Bonvin AM, Langedijk JP, Davis D, Forsman Quigley A, Aasa-Chapman MM, Seaman MS, Ramos A, Poignard P, Favier A, Simorre JP, Weiss RA, Verrips CT, Weissenhorn W, Rutten L (2013) A gp41 MPER-specific llama VHH requires a hydrophobic CDR3 for neutralization but not for antigen recognition. PLoS Pathog 9:e1003202.
75. Frey G, Peng H, Rits-Volloch S, Morelli M, Cheng Y, Chen B (2008) A fusion-intermediate state of HIV-1 gp41 targeted by broadly neutralizing antibodies. Proc Natl Acad Sci USA 105:3739–3744.
76. Cavacini LA, Duval M, Robinson J, Posner MR (2002) Interactions of human antibodies, epitope exposure, antibody binding and neutralization of primary isolate HIV-1 virions. AIDS 16:2409–2417.
77. Leaman DP, Kinkead H, Zwick MB (2010) In-solution virus capture assay helps deconstruct heterogeneous antibody recognition of human immunodeficiency virus type 1. J Virol 84:3382–3395.
78. Kessans SA, Linhart MD, Matoba N, Mor T (2013) Biological and biochemical characterization of HIV-1 Gag/dgp41 virus-like particles expressed in Nicotiana benthamiana. Plant Biotech J 11:681–690.
79. Markwell MA, Haas SM, Bieber LL, Tolbert NE (1978) A modification of the Lowry procedure to simplify protein determination in membrane and lipoprotein samples. Anal Biochem 87:206–210.
80. Schägger H (2006) Tricine-SDS-PAGE. Nat Protoc 1: 16–22.
81. Lawrence RM, Varco-Merth B, Bley CJ, Chen JJ, Fromme P (2011) Recombinant production and purification of the subunit c of chloroplast ATP synthase. Protein Expr Purif 76:15–24.
82. Song L, Wang Z, Zhou D, Nand A, Li S, Guo B, Wang Y, Cheng Z, Zhou W, Zheng Z, Zhu J (2013) Waveguide coupled surface plasmon resonance imaging measurement and high-throughput analysis of bio-interaction. Sensors Actuators B: Chem 181:652–660.